1	
2	Janus Membrane with a Dense Hydrophilic Surface Layer for
3	Robust Fouling and Wetting Resistance in Membrane Distillation
4	New Insight into Wetting Resistance
	Trow morght into Wotting Roolotanoo
5	
6	Environmental Science & Technology
7	
8	Revised: September 10 2021
9	
10	Dejun Feng ^{a,1} , Yuanmiaoliang Chen ^{c,1} , Zhangxin Wang ^{a,b,*} ,
11	Shihong Lind,e,*
12	
13	^a Key Laboratory for City Cluster Environmental Safety and Green
14 15 16	Development of the Ministry of Education, Institute of Environmental and Ecological Engineering, Guangdong University of Technology, Guangzhou, 510006, China
17	^b Guangdong Provincial Key Laboratory of Water Quality Improvement and
18	Ecological Restoration for Watershed, Institute of Environmental and Ecological
19	Engineering, Guangdong University of Technology, Guangzhou, 510006, China
20	^c NUS Graduate School for Integrative Science and Engineering, National
21	University of Singapore, Singapore, 119077, Singapore
2223	^d Department of Civil and Environmental Engineering, Vanderbilt University Nashville, Tennessee 37235-1831, United States
24	eDepartment of Chemical and Biomolecular Engineering, Vanderbilt
25	University, Nashville, Tennessee 37235-1831, United States
26	Omversity, indstrute, femicisee 37233 1031, Omited States
27	¹ These authors contribute equally to this work.
28	Corresponding author: email: <u>zhangxin.wang@gdut.edu.cn</u> ;
29	shihong.lin@vanderbilt.edu; Tel: +1 (615) 322-7226
30	

ABSTRACT

Although membrane distillation (MD) has been identified as a promising technology to treat hypersaline wastewaters, its practical applications face two prominent challenges: membrane wetting and fouling. Herein, we report a facile and scalable approach for fabricating a Janus MD membrane comprising a dense polyvinyl alcohol (PVA) surface layer and a hydrophobic polyvinylidene fluoride (PVDF) membrane substrate. By testing the Janus membrane in direct contact MD experiments using feeds containing sodium dodecyl sulfate (SDS) surfactant or/and mineral oil, we demonstrated that the dense Janus membrane can simultaneously resist wetting and fouling. This method represents the simplest approach to date for fabricating MD membranes with simultaneous wetting and fouling resistance. Importantly, we also unveil the mechanism of wetting resistance by measuring breakthrough pressure and surfactant permeation (through the PVA layer) and found that wetting resistance imparted by a dense hydrophilic layer is attributable to capillary pressure. This new insight will potentially change the paradigm of fabricating wetting resistant membranes and enable robust applications of MD and other membrane contactor processes facing challenges of pore wetting or/and membrane fouling.

KEYWORDS

- 48 Membrane distillation, Desalination, Wetting, Fouling, Surface modification, Hydrophilic coating,
- 49 Capillary pressure

SYNOPSIS

- A new understanding of wetting resistance enables a simple and scalable approach of fabricating
- 53 robust membranes for membrane distillation.

INTRODUCTION

Intensified global freshwater scarcity imposes growing demands on wastewater treatment.^{1, 2} Membrane distillation (MD) is an emerging thermal desalination technology that is promising to treat highly saline wastewaters.^{3, 4} The key component in a typical MD system is a microporous hydrophobic membrane that separates the hot feed and cold distillate streams. In an MD process, the temperature difference-induced partial vapor pressure difference drives the water vapor to transport through the membrane pores from the feed stream to the distillate stream, while the non-volatile species (e.g., salts) are rejected and remain in the feed stream. Compared to the state-of-the-art thermal desalination technology, mechanical vapor compression (MVC), MD is potentially cheaper in capital cost and can leverage low-grade thermal energy (e.g., industrial waste heat and geothermal energy) instead of electricity.⁵⁻⁷ Recently, MD has been proposed for off-grid applications because of its small footprint.^{8, 9}

Membrane wetting and fouling are two prominent challenges in practical MD applications.^{10,}
¹¹ Membrane wetting is caused by amphiphilic contaminants that reduce the liquid entry pressure (LEP) of the membrane pores and lead to the direct penetration of feed water through the membrane.^{12, 13} As a result of membrane wetting, salt rejection is substantially compromised. Membrane wetting is a major hurdle for MD to treat wastewaters containing surfactants (e.g., most industrial wastewaters).^{14, 15} Membrane fouling occurs as the foulants attach to the membrane surface, block the membrane pores, and lead to a significant flux decline. When MD is applied to treat wastewaters containing abundant hydrophobic contaminants (e.g., shale gas/oil wastewaters),^{16, 17} membrane fouling is a particular concern because of the strong hydrophobic-hydrophobic interaction.^{18, 19}

To overcome membrane wetting and fouling, novel MD membranes with special wettability have been employed. ²⁰⁻²³ Specifically, omniphobic MD membranes that are resistant to wetting by low-surface-tension liquids have been proposed for wetting mitigation, ²⁴⁻²⁶ and composite MD membranes with a superhydrophilic surface layer and a hydrophobic substrate have been developed for fouling mitigation. ²⁷⁻²⁹ Since the compositions of industrial brines are usually complex, membrane wetting and fouling could occur simultaneously. However, based on previous studies, ^{10, 11} neither omniphobic nor composite MD membranes can resist membrane wetting and fouling at the same time. To achieve simultaneous wetting and fouling resistance, Janus MD membranes comprising a superhydrophilic surface layer and an omniphobic membrane substrate

have been developed.^{30, 31} However, the fabrication of Janus membranes with omniphobic substrates is complicated, hindering the adoption of such membranes in practical applications.

Inspired by nanofiltration (NF) membranes that can remove surfactants from wastewaters due to the size exclusion effect,^{32, 33} an NF/MD membrane composed of a dense top layer and a polyvinylidene fluoride (PVDF) substrate has been developed very recently.³⁴ The as-developed NF/MD membrane showed an excellent resistance to both membrane wetting and fouling. However, despite the absence of omniphobic substrate, the fabrication of the NF/MD membrane is still difficult to scale up because of the inverted co-deposition of hydrophilic polymer and use of sodium-functionalized carbon quantum dots. Therefore, an alternative approach to fabricate a robust MD membrane with simultaneous wetting and fouling resistance is still needed. More importantly, beyond the specific membrane fabrication approach, the mechanism of wetting and fouling resistance of the as-fabricated MD membrane needs to be elucidated, as it can provide critical guidance to the future membrane development.

In this study, we report a facile and scalable approach of fabricating a Janus MD membrane comprised of a dense PVA layer and a hydrophobic PVDF membrane substrate. The morphology and wettability of the as-fabricated Janus membrane are characterized. We then conduct DCMD experiments with a saline feed containing surfactants to investigate the wetting resistance of the dense PVA/PVDF Janus membrane. The mechanism of wetting resistance is elucidated by probing the surfactant permeability of the membrane via diffusion experiment and determining the breakthrough pressure of the membrane with an ethanol-water mixture. We further conduct direct contact membrane distillation (DCMD) experiments with an oily saline feed to investigate the fouling resistance of the dense PVA/PVDF Janus membrane. The mechanism of fouling resistance is elucidated by measuring the underwater oil-membrane interaction via force spectroscopy. Finally, we conduct DCMD experiments with a saline feed containing both surfactants and oil to demonstrate the simultaneous wetting and fouling resistance of the dense PVA/PVDF Janus membrane.

MATERIALS AND METHODS

Materials and Chemicals. The substrate membranes used in this study were commercial PVDF membranes (0.45 μm, Merck Millipore Ltd.). Polyvinyl alcohol (PVA, M_w≈67,000), poly (acrylic acid-co-2-acrylamido-2-methyl propanesulfonic acid) (P(AA-AMPS), 98%), sodium

dodecyl sulfate (SDS, 99%), ethanol (99.5 %, v/v), and humic acid were purchased from Aladdin, China. Sodium chloride (NaCl) and sulfuric acid (H₂SO₄, 98%) were acquired from Guangzhou chemical reagent factory, China. Polyethylene glycols (PEG, Mw = 400, 600, 2000, and 4000 Da) were obtained from Macklin Co. Ltd, China.

Fabrication of Dense PVA/PVDF Janus Membrane. A homogeneous PVA solution was obtained by adding 1.1g PVA to 98 mL deionized (DI) under vigorous stirring at 90 °C for 2 hours. The pH of the PVA solution was adjusted to 1 using a 1.0 M H₂SO₄ aqueous solution. After pH adjustment, 0.9 g P(AA-AMPS) was added to the PVA solution as the crosslinker. The PVA-P(AA-AMPS) dope solution was prepared after P(AA-AMPS) being completely dissolved under stirring at room temperature.

The dense PVA/PVDF Janus membrane was prepared via spray coating (Figure 1).³⁵ Specifically, 5 mL PVA-P(AA-AMPS) dope solution was sprayed onto a 6.5 cm × 1.5 cm PVDF membrane substrate using a spray gun. The spraying pressure was controlled at 0.1 MPa. The dope solution-sprayed PVDF membrane was heated at 100 °C for 15 mins in a muffle furnace to facilitate the crosslinking of PVA. After being cooled down at room temperature and soaked in deionized (DI) water for 24 h to remove soluble impurities and residual acids, the dense PVA/PVDF Janus membrane was ready for testing.

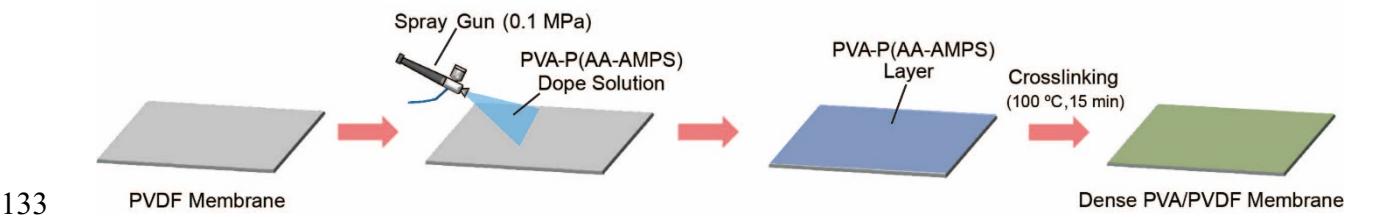


Figure 1. Schematic illustration of the fabrication of a dense PVA/PVDF Janus membrane.

Membrane Characterizations. The surface morphology of the pristine PVDF membrane and dense PVA/PVDF Janus membrane was observed using scanning electron microscopy (SEM, Tescan, LTRA 3 XMU). The pore size distribution of the PVA layer was measured using the solute filtration method (detailed procedures reported in the Supporting Information).³⁴ The chemical composition of the dense membrane was verified with attenuated total reflection-Fourier transform infrared spectroscopy (ATR-FTIR, IRTracer-100, Shimadzu). The surface wettability of the dense PVA/PVDF Janus membrane was characterized by measuring the static contact angles (CA) using

an optical tensiometer (Attension Theta Lite, Biolin Scientific). Both the in-air water CA and underwater oil CA (with mineral oil) were measured. Specifically, the in-air water CA was determined using the sessile drop method, and the underwater oil CA was determined using the captive bubble method by replacing the air bubble with a mineral oil droplet.

Evaluation of Wetting and Fouling Resistance. Direct contact MD (DCMD) experiments were used to evaluate the performance of the pristine PVDF membrane and the dense PVA/PVDF Janus membrane. The schematic of the system setup can be found in Supporting Information. In all DCMD experiments, the temperatures of the feed and distillate were maintained to be 60 and 20 °C, respectively, while the flow rates of feed and distillate streams were controlled at 0.8 L/min and 0.4 L/min, respectively, resulting in a larger hydraulic pressure on the feed side to facilitate the detection of membrane wetting (as wetting will unequivocally results in flux increase under this condition). The cumulative mass and the conductivity of the distillate stream were constantly recorded, from which the real-time vapor flux and salt rejection can be obtained (Details in Supporting Information). For DCMD experiments with the dense PVA/PVDF Janus membrane, the dense PVA layer was facing the feed.

The wetting tests were carried out using a saline feed containing 35 g L⁻¹ NaCl and SDS surfactant. In each test, the wetting agent, SDS, was incrementally added to the saline feed every 2 h. After each addition, the SDS concentration in the feed increased by 0.05 mM. The wetting test was terminated once the membrane was wetted as indicated by both increases of distillate conductivity and measured water flux (flux increased due to direct liquid permeation under a pressure difference from the feed to distillate). Otherwise, the experiments were terminated when the SDS concentration reached 0.2 mM.

The fouling tests were conducted using an oily saline feed containing 35 g L⁻¹ NaCl and 2,000 ppm mineral oil. Instead of using hydrophilic natural organic contaminants (e.g., humic acids), mineral oil was selected as the model foulant not only because of its relevance in oil and gas wastewater management but also because hydrophobic MD membranes are more prone to the fouling induced by the hydrophobic contaminants due to the strong hydrophobic-hydrophobic interaction underwater (Figure S3 in the Supporting Information).³⁶ Therefore, the MD membranes were challenged to a greater extent by using mineral oil as a fouling agent. The feed was prepared by vigorously mixing 2 g mineral oil and 1 L NaCl aqueous solution at 16,500 rpm for 20 min using a homogenizer (FJ200-SH, Huxishiye). No obvious phase separation was observed during

the whole fouling tests. Based on dynamic light scattering (DLS) measurements, the oily saline feed showed an average oil droplet size of $1.63 \pm 0.35 \,\mu m$ (Figure S4 in Supporting Information).

The simultaneous wetting and fouling tests were performed using an oily saline feed containing 35 g L⁻¹ NaCl, 0.1 mM SDS, and 1,000 ppm mineral oil. Like the oily saline feed used for fouling tests, the oily saline feed used for simultaneous wetting and fouling tests was prepared by vigorously mixing 0.029 g SDS, 1 g mineral oil, and 1 L NaCl aqueous solution at 16,500 rpm for 20 min using a homogenizer (FJ200-SH, Huxishiye). The averaged oil droplet size in the asprepared feed was measured to be 0.78 \pm 0.17 μm using DLS (Figure S4 in Supporting Information), which suggests that SDS promotes the formation of more finely dispersed oil droplets. For the long-term test with the dense PVA/PVDF Janus membrane, the membrane was rinsed with DI water for 15 min every 30 hours.

Force Spectroscopy Measurement. To directly measure the underwater oil-membrane interactions, oil-probe force spectroscopy was performed using a force tensiometer (DCAT21, Dataphysics).^{28, 37, 38} For each measurement, a small membrane coupon was immobilized at the bottom of a glass cell using a double-sided tape, and then the cell was filled with DI water. In the glass cell, a mineral oil droplet (~10 μL) was hung onto a homemade Titanium force probe underwater (Figure S5 in Supporting Information). During each measurement, the force probe approached the membrane surface at a constant speed of 0.3 mm min⁻¹, and once the oil droplet was in contact with the membrane, retracted from the membrane surface at the same constant speed. The force applied on the force probe was measured by a micro-electro-mechanical sensor and recorded as a function of the force probe displacement.

Diffusion Experiment. Diffusion experiments were conducted to determine the permeability of SDS through the pristine PVDF membrane and dense PVA/PVDF Janus membrane.³⁹ In each diffusion experiment, a small membrane coupon with an area of 2.27 cm² was assembled into custom-made two-chamber diffusion cell after being wetted by ethanol and rinsed by DI water (Figure S6 in Supporting Information). The two chambers of the diffusion cell were filled with 5 mM SDS aqueous solution and DI water, respectively. The solution conductivity in the DI water chamber was constantly monitored over time. The permeability of SDS was indicated by the time-dependent SDS concentration obtained from the conductivity data.

Breakthrough Pressure Measurement. The breakthrough pressure of the pristine PVDF membrane and dense PVA/PVDF Janus membrane with an ethanol-water mixture were

determined using a crossflow ultrafiltration cell (Figure S7 in Supporting Information). The surface tension of the ethanol-water mixture was kept the same as that of the saline feed with 0.2 mM SDS in the wetting tests (Details can be found in the later discussion and Supporting Information). During each test, the hydraulic pressure of the ethanol-water mixture stream was incrementally raised by a gear pump and determined by a pressure gauge. Once liquid permeation through the membrane was observed, the applied hydraulic pressure was recorded as the breakthrough pressure.

RESULTS AND DISCUSSION

Membrane Characterizations. The morphologies of the pristine PVDF membrane and dense PVA/PVDF Janus membrane were revealed by SEM. Micron-sized pores were observed on the surface of the pristine PVDF membrane (Figure 2A) but not the Janus membrane coated with a PVA layer (Figure 2B), because a relatively dense PVA layer formed on the surface of the PVDF membrane. The morphologies of the bottom surface (Figure 2C) and cross-section (Figure 2D) of the Janus membrane suggest that the PVA coating only affects the morphology of the top surface of the PVDF membrane and results in an asymmetric structure composed of a thin surface layer of PVA and a thick substrate made of the original PVDF membrane. Such a structure is achieved because the hydrophobicity of the PVDF membrane substrate prevented the deep penetration of PVA solution in the membrane fabrication process. However, the partial (and thin) penetration of the PVA layer into the PVDF substrate (Figure 2D) provides strong anchoring of the dense surface coating layer to the porous PVDF membrane substrate. Additionally, the pore size distribution of the PVA layer is below 4 nm with a mean value of 1.25 nm (Figure 2E), which is two orders of magnitude smaller than the nominal pore size of the PVDF substrate (0.45 μm).

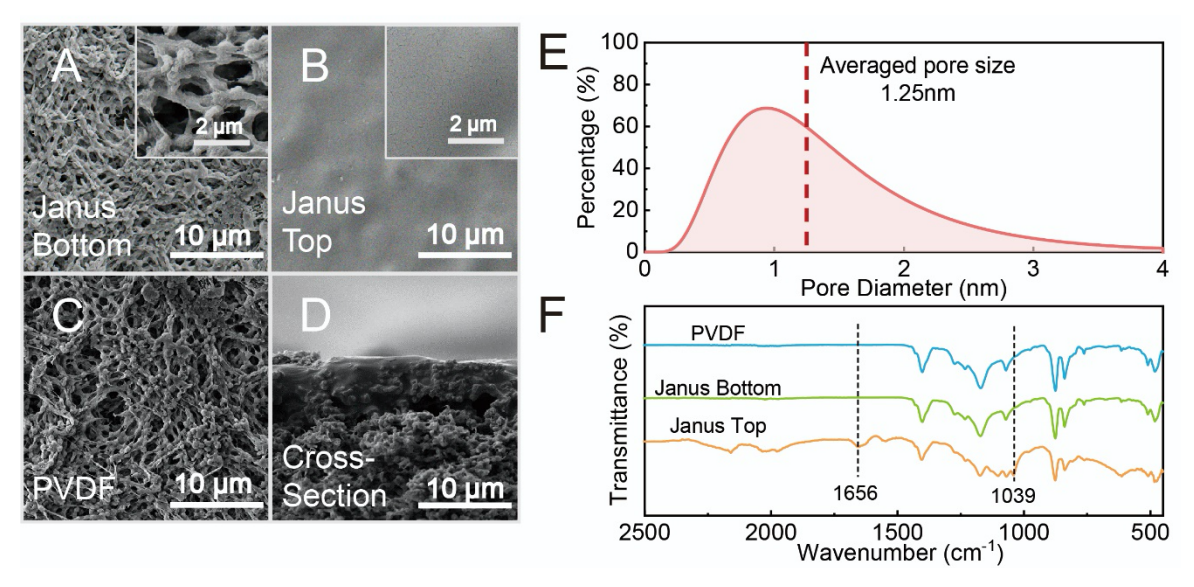


Figure 2. Morphology of the dense PVA/PVDF Janus membrane. SEM images featuring the morphologies of (A) a pristine PVDF membrane surface, (B) the top surface of the Janus membrane (i.e., the PVA layer), (C) the bottom surface of the Janus membrane (i.e., the PVDF substrate), and (D) the cross-section view of the Janus membrane. The insets in panels (A) and (B) feature the local morphologies at a larger magnification. (E) Pore size distribution of the PVA layer. The dashed line refers to the mean pore size of the PVA layer. (F) ATR-FTIR spectra of the pristine PVDF membrane (blue curve), the bottom surface of the Janus membrane (green curve), and the top surface of the Janus membrane (orange curve).

ATR-FTIR spectra were used to validate the chemical compositions of the dense PVA/PVDF Janus membrane (Figure 2F). The spectra of the pristine PVDF membrane (blue curve) and the bottom surface of the Janus membrane (green curve) are the same, which confirms that the bottom of the Janus membrane is simply PVDF. In comparison, the spectrum of the top surface of the Janus membrane (orange curve) shows two new peaks characteristic of PVA at wavenumbers of 1,656 and 1,039 cm⁻¹, which correspond to the stretched vibrations of C=O and S-O, respectively³⁵, Therefore, ATR-FTIR spectra further verifies the successful fabrication of the dense PVA/PVDF Janus membrane.

The wetting behaviors of the top and bottom surfaces of the dense PVA/PVDF Janus membrane were observed with three liquids, including water, ethanol, and mineral oil (Figure 3A). All three liquids spread on the top surface of the dense PVA/PVDF Janus membrane (i.e., the dense PVA layer), but the membrane substrate was not wicked through likely because the PVA layer that is too dense for the liquids to penetrate through. In contrast, although water beads up on the bottom surface of the dense PVA/PVDF Janus membrane (i.e., the pristine PVDF membrane substrate), the membrane was immediately wetted and wicked through by ethanol and mineral oil

because low-surface-tension liquids would result in a low or even negative liquid entry pressure (LEP) of the membrane pores, consequently leading to membrane wetting.^{41, 42} The drastically different wetting phenomena on the two sides of the dense PVA/PVDF Janus membrane suggest that PVA surface coating could potentially mitigate membrane wetting by preventing the wetting agents from reaching the hydrophobic membrane substrate.

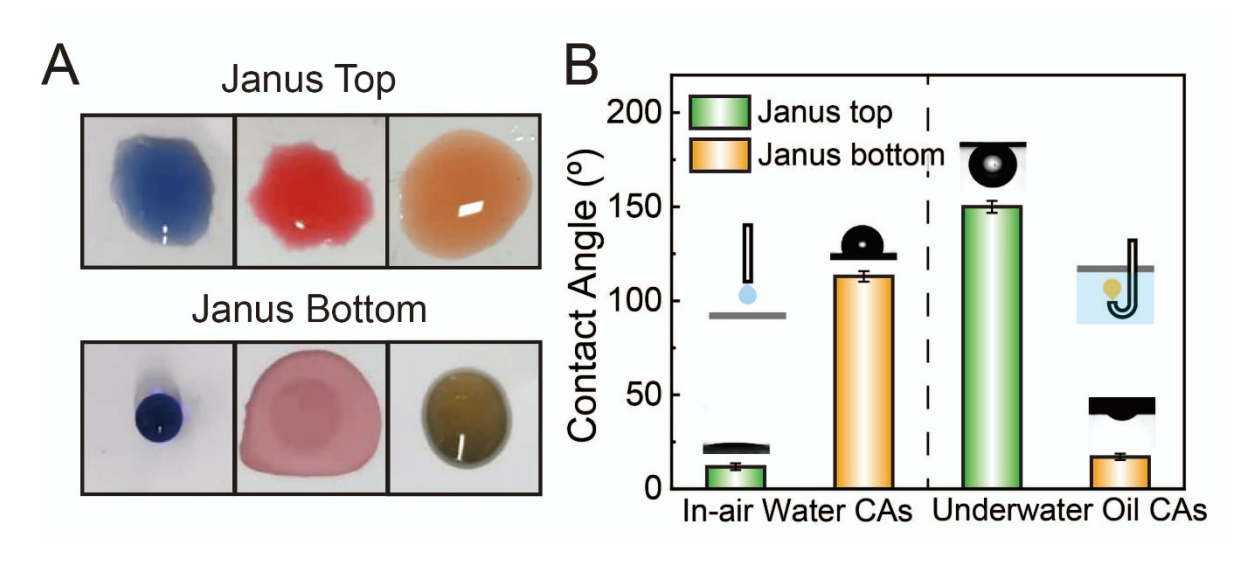


Figure 3. Wettability of the dense PVA/PVDF Janus membrane. (A) Photographic images of three different liquids (i.e., water, ethanol, and mineral oil) on the top and bottom surfaces of the dense PVA/PVDF Janus membrane. For the purpose of differentiation, water, ethanol, and mineral oil were dyed to blue, red, and orange colors, respectively. (B) Contact angles (CA) for the top (green columns) and bottom (orange columns) surfaces of the dense PVA/PVDF Janus membrane with water in air (left) and with oil underwater (right). The insets denote the two different CA measurement methods.

The wettability of the dense PVA/PVDF Janus membrane was further quantified by contact angle (CA) measurements (Figure 3B). The top surface of the dense PVA/PVDF Janus membrane is highly superhydrophilic with a water CA of $11.83 \pm 1.81^{\circ}$, whereas the bottom surface of the dense PVA/PVDF Janus membrane is hydrophobic with a water CA of $113.2 \pm 2.26^{\circ}$. The CA measurements confirm the asymmetric wettability of the dense PVA/PVDF Janus membrane. To acquire information that is directly relevant to membrane fouling, underwater oil CAs of the dense PVA/PVDF Janus membrane were determined. The top surface of the dense PVA/PVDF Janus membrane presents excellent underwater oleophobicity with a large oil CA of $150.42 \pm 2.78^{\circ}$ (Figure 3A). Such underwater oleophobicity implies that the dense PVA/PVDF Janus membrane can effectively resist oil adhesion and wetting in MD operation. In comparison, the bottom surface

of the dense PVA/PVDF Janus membrane is underwater oleophilic with a small oil CA of $17.35 \pm 1.73^{\circ}$, implying a high fouling propensity of the pristine PVDF membrane when exposed to mineral oil under water.

Wetting Resistance of the dense PVA/PVDF Janus Membrane. The pristine PVDF membrane and dense PVA/PVDF Janus membrane were challenged by saline feeds containing SDS surfactant to evaluate their wetting resistance. Soon after the addition of 0.05 mM SDS in the feed solution, the pristine PVDF membrane was wetted, indicated by the rapidly increased vapor flux and drastically decreased salt rejection (Figure 4A). This observation is consistent with the observation that low-surface-tension liquids (e.g., ethanol and mineral oil) could readily wet a PVDF membrane (Figure 3A), except that in the MD wetting experiment the surface tension of the feed solution was reduced by the addition of SDS. The wetted membrane pores allowed direct permeation of the feed solution in its liquid form, resulting in an increase of the apparent flux (a combination of vapor flux through unwetted pores and liquid flux through wetted pores) and a decrease of the salt rejection.

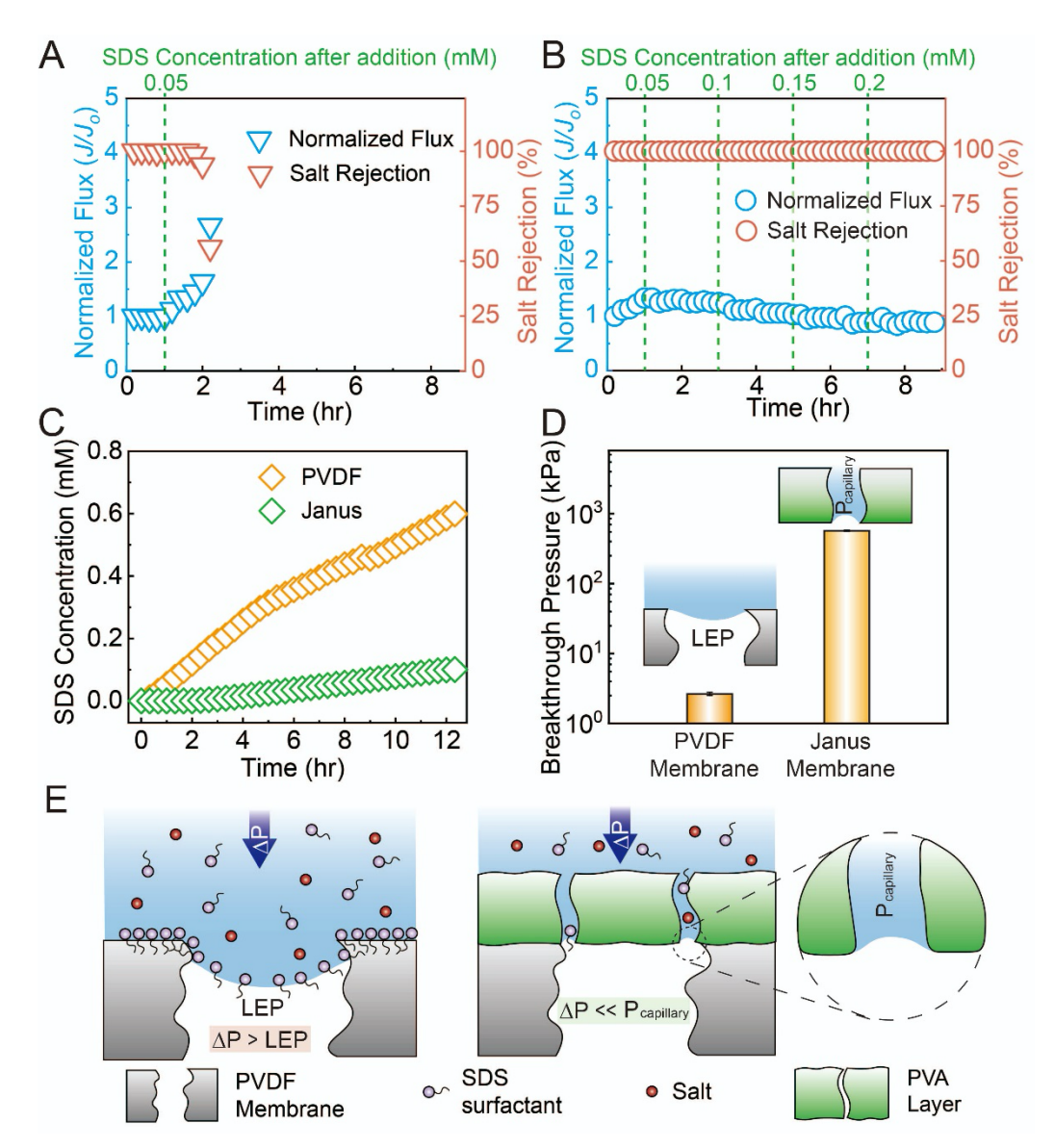


Figure 4. Wetting resistance of the dense PVA/PVDF Janus membrane. Normalized vapor flux, J/J_0 (blue left vertical axis), and salt rejection rate (orange right vertical axis) for (A) the pristine PVDF membrane and (B) Janus membrane in DCMD wetting experiments. The initial feed was 35 g/L NaCl solution, and the green dashed lines denote the addition of SDS with the SDS concentration after addition indicated on the top. The feed and permeate temperatures were set at 60 and 20 °C, respectively, while the flow rates of feed and permeate streams were controlled at 0.8 L/min and 0.4 L/min, respectively. The initial vapor fluxes, J_0 , in panels (A) and (B) were 23.31 ± 2.25 and 24.18 ± 2.01 L m⁻² h⁻¹, respectively. (C) SDS concentration in receiving solution (started as DI water) contacting the pristine PVDF membrane (orange diamonds) and dense PVA/PVDF Janus membrane (green diamonds) in the diffusion experiment. The opposite side of the membrane was in contact with a 5 mM SDS solution. (D) Breakthrough pressures of the pristine PVDF membrane (orange column) and dense PVA/PVDF Janus membrane (green column) with an ethanol-water mixture. The surface tension of the ethanol-water mixture was the same as that of saline feed with 0.2 mM SDS (~36 mN/m). The insets represent the origins of the breakthrough pressures of the two membranes. (E) Schematic illustrations of the wetting and anti-

wetting mechanisms of the pristine PVDF membrane (left) and dense PVA/PVDF Janus membrane (right), respectively.

In comparison, the dense PVA/PVDF Janus membrane showed an outstanding wetting resistance with a stable vapor flux and nearly perfect salt rejection even after the addition of 0.2 mM SDS in the feed solution (Figure 4B). The outstanding wetting resistance of the dense PVA/PVDF Janus membrane is consistent with the wetting behavior shown in Figure 3A. Like ethanol and mineral oil, the low-surface-tension SDS solutions could not permeate through the dense PVA layer, and thereby the PVDF membrane substrate can remain unwetted and sustain a stable DCMD performance. Notably, despite the very different surface morphologies (Figures 2A and B), the initial vapor fluxes of the pristine PVDF membrane and dense PVA/PVDF Janus membrane were almost the same, which is consistent with what have been observed in previous studies.⁴³⁻⁴⁵

In the recent literature, size exclusion effect is considered as the major mechanism of wetting resistance for MD membranes with a dense surface layer. 34,46 Specifically, it was argued that the permeation of SDS through the dense layer is prevented because the pores in the dense layer are too small for SDS to enter. To verify this explanation, diffusion experiment was conducted to probe the SDS permeability of the pristine PVDF membrane and dense PVA/PVDF Janus membrane. The results from the diffusion experiments (Figure 4C) clearly suggest that SDS can permeate through the dense PVA layer. Furthermore, the SDS permeability of the PVA/PVDF Janus membrane is $\sim 1/5$ of that of the pristine PVDF membrane. If size exclusion were the major mechanism of wetting resistance, the dense PVA/PVDF Janus membrane would still be wetted with a prolonged test time or/and an increased SDS concentration, which is inconsistent with the wetting test results (Figures 4A and B). In addition, the SDS rejection rate of the dense PVA/PVDF Janus membrane in filtration was only 84.43 ± 1.42 % (details in the Supporting Information). which further confirms that size exclusion effect cannot explain the outstanding wetting resistance of the dense PVA/PVDF Janus membrane.

To elucidate the mechanism of wetting resistance of the dense PVA/PVDF Janus membrane, the breakthrough pressures of the pristine PVDF membrane and Janus membrane were determined with an ethanol-water mixture. The SDS-containing feed solution was not used to determine the breakthrough pressure because the breakthrough pressure with the SDS feed was similar to that with DI water (Figure S7 in Supporting Information). Such a phenomenon is attributable to the

adsorption of SDS onto the PVDF membrane surface at the solution-membrane-air interface (i.e., wetting frontier). 47,48 During the breakthrough pressure measurement, the replenishment of SDS from the bulk feed to the wetting frontier is far slower than the adsorption rate of SDS, leading to a substantially declined SDS concentration at the wetting frontier. The declined SDS concentration renders the surface tension of the wetting fronter similar to that of DI water, consequently leading to similar breakthrough pressures with the SDS feed and with DI water. Alternatively, another low-surface-tension liquid, an ethanol-water mixture, was used in the breakthrough pressure measurements due to its ability to maintain a relatively constant surface tension during the measurements. Compared to the breakthrough pressures determined with the SDS-containing feed solution, the breakthrough pressures determined with the ethanol-water mixture are more relevant to the membrane wetting in prolonged MD experiments. To relate the measured breakthrough pressures to the results of wetting experiments, the surface tension of the ethanol-water mixture was controlled to be the same as that of the saline feed containing 0.2 mM SDS (i.e., the highest SDS concentration in the wetting experiments).

The breakthrough pressures of the PVDF membrane and dense PVA/PVDF Janus membrane with the ethanol-water mixture were measured to be 2.7 ± 0.2 and 570.0 ± 10.0 kPa, respectively (Figure 4D). The measured breakthrough pressures suggest that the PVDF membrane could be easily penetrated through by the ethanol-water mixture, whereas the dense PVA/PVDF Janus membrane exhibited strong resistance to the penetration by the ethanol-water mixture. The drastic difference between breakthrough pressures of the two membranes is, at first sight, surprising. Based on the equation for predicting LEP, a hydrophilic porous matrix should have a negative LEP, which suggests spontaneous wetting. Our measurements, however, suggest that the Janus membrane with a hydrophilic PVA layer is substantially more difficult to penetrate through than the hydrophobic PVD membrane. The key to resolve this conundrum is to recognize that penetration of a liquid through a porous membrane requires not only entry into the porous matrix but also exit from the same matrix.

For a symmetric hydrophobic PVDF membrane, the breakthrough pressure is the LEP, because once the liquid enters the membrane pores, it can readily flow out. As the PVDF membrane with relatively large pores has a small LEP with a low-surface-tension liquid, its breakthrough pressure with the ethanol-water mixture is very small. In contrast, while the dense hydrophilic PVA layer is spontaneously wicked via capillary force, pushing water out of the same

layer is challenging due to the exact same capillary force.^{49, 50} Thus, the breakthrough pressure of the Janus membrane is the capillary pressure in the dense PVA layer. Based on the Young-Laplace equation, the capillary pressure in the dense PVA layer is very large because of the strong hydrophilicity of PVA and the very small pore size.^{51, 52} Therefore, the breakthrough pressure of the dense PVA/PVDF Janus membrane is very large.

From the diffusion experiment and breakthrough pressure measurement, the mechanism of wetting resistance of the dense PVA/PVDF Janus membrane becomes evident and is illustrated in Figure 4E. For the PVDF membrane, adding SDS to the feed reduces the surface tension of the feed solution, resulting in a declined LEP of the hydrophobic membrane. Once the hydraulic pressure applied in the MD operation exceeds the LEP, the SDS-containing feed solution starts to intrude into the membrane pore and consequently leads to membrane wetting. For the dense PVA/PVDF Janus membrane, the SDS-containing feed solution can easily wick the dense PVA layer because of the strong capillary force. However, for the SDS-containing feed solution to exit the dense PVA layer and wet the underlying PVDF substrate, the same capillary needs to be overcome. Since the capillary pressure in the dense PVA layer is several orders of magnitude larger than the hydraulic pressure applied in MD operations, the SDS-containing feed solution is retained by the PVA layer and the PVDF membrane substrate can thus remain unwetted. Therefore, by trapping the SDS-containing feed solution in the dense PVA layer using capillary force, the dense PVA/PVDF Janus membrane can effectively mitigate membrane wetting in MD operations.

Fouling Resistance of the dense PVA/PVDF Janus Membrane. Both the pristine PVDF membrane and dense PVA/PVDF Janus membrane were tested in direct contact MD (DCMD) experiments using a saline feed containing mineral oil. As shown in Figure 5A, the vapor flux of the pristine PVDF membrane declined rapidly shortly after the start of the experiment, indicating that the membrane was severely fouled by mineral oil. As the pristine PVDF membrane is underwater oleophilic (Figure 3B), mineral oil droplets tend to attach to and spread on the membrane surface, thereby blocking the membrane pores and leading to the decline of vapor flux.²⁸ Salt rejection was not compromised as oil fouling alone did not result in pore wetting.

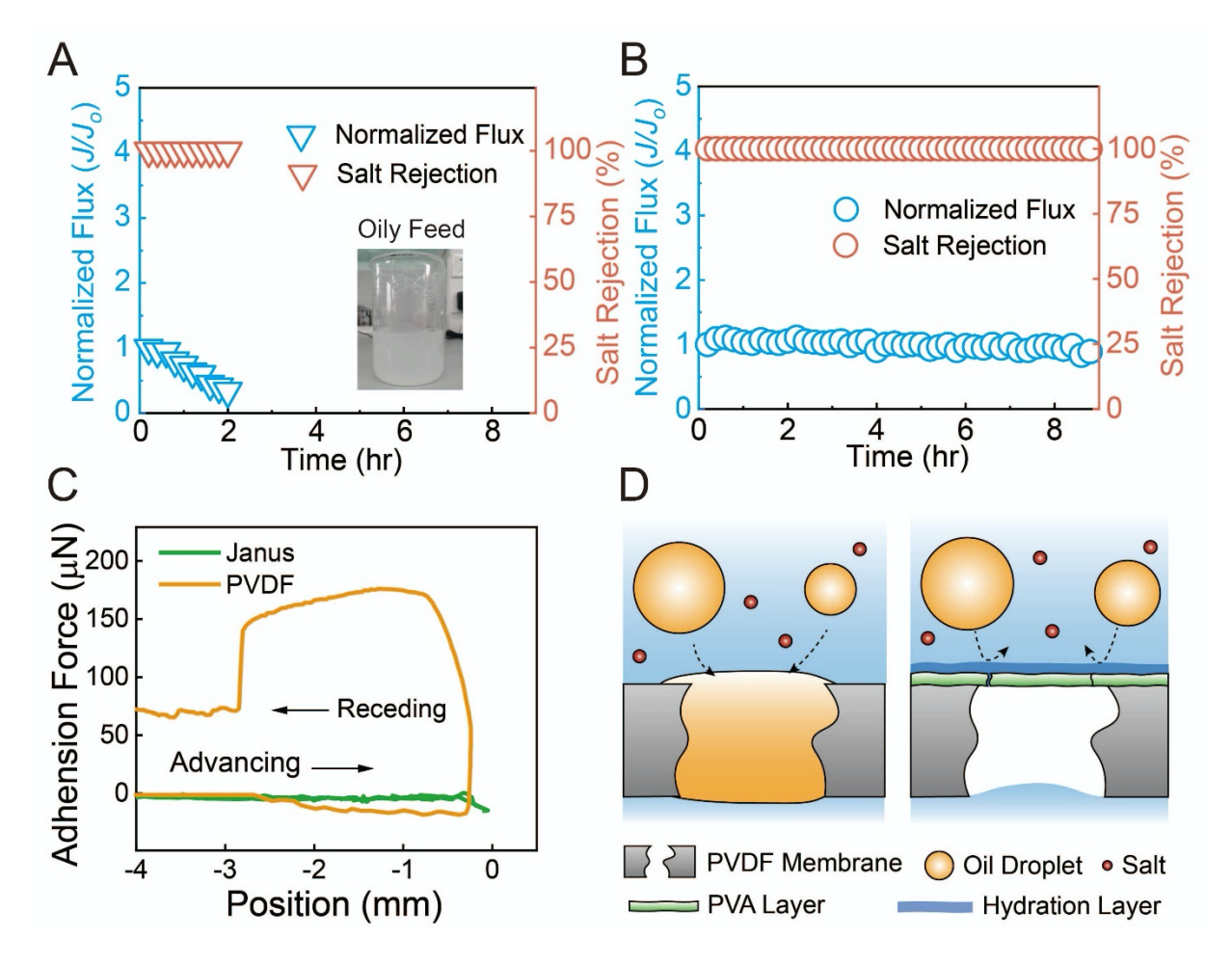


Figure 5. Fouling resistance of the dense PVA/PVDF Janus membrane. Normalized vapor flux, J/J_0 , (blue left vertical axis) and salt rejection rate (red right vertical axis) for (A) the pristine PVDF membrane and (B) dense PVA/PVDF Janus membrane in DCMD fouling tests. The feed was saline oil-in-water emulsion with 35 g/L NaCl and 2000 ppm mineral oil (inset in panel A). The feed and permeate temperatures were set at 60 and 20 °C, respectively, while the flow rates of feed and permeate streams were controlled at 0.8 L/min and 0.4 L/min, respectively. The initial vapor fluxes, J_0 , in panels (A) and (B) were 25.34 \pm 2.51 and 24.29 \pm 1.93 L m⁻² h⁻¹, respectively. (C) Force curves for the interactions of a mineral oil droplet with the pristine PVDF membrane (orange curve) and dense PVA/PVDF Janus membrane (green curve). (D) Schematic illustrations of the mechanism of fouling for the pristine PVDF membrane (top) and the mechanism of fouling resistance for the dense PVA/PVDF Janus membrane (bottom), respectively.

In contrast, the PVA/PVDF Janus membrane was able to maintain a relatively stable vapor flux and perfect salt rejection over 9 hours (Figure 5B), suggesting an excellent fouling resistance. The fouling resistance is in accordance with the underwater oil CA measurement. Since the dense PVA surface coating is highly underwater oleophobic, the oil droplets cannot adhere to and spread on the PVA-coated membrane surface, leaving the membrane pores intact for vapor transport and salt rejection.

To better understand the anti-fouling mechanism of the dense PVA/PVDF Janus membrane, force spectroscopy was performed to unveil the interaction between the pristine PVDF membrane and dense PVA/PVDF Janus membrane. As shown in Figure 5C, each force curve comprises an advancing stage and a receding stage. In the advancing stage, the oil droplet approached the membrane surface without oil-membrane contact. As soon as the oil droplet touched the membrane, it retracted from the membrane surface, which marks the start of the receding stage.

The force curves in the advancing stage were similar for both the pristine PVDF membrane and dense PVA/PVDF Janus membrane, recording a zero "adhesion force" due to the lack of interaction between the oil and the membrane. Once the oil droplet touched the membrane surface, a strong adhesion force was observed with the PVDF membrane, indicating a strong oil-membrane attraction. Such an attraction can be attributed to the strong hydrophobic interaction between the oil droplet and the PVDF membrane underwater. ^{18, 19} In stark contrast, no adhesion force was observed for the dense PVA/PVDF Janus membrane upon the contact of the oil droplet and the membrane surface, suggesting the lack of oil-membrane attraction. The highly hydrophilic PVA layer introduces a hydration layer that it is energetically unfavorable for the adhesion and spreading of oil droplets. ^{28, 53}

In the receding stage, an abrupt decrease was observed on the force curve for the interaction with the PVDF membrane. Such a decrease was caused by the split of the oil droplet upon the oil detachment from the membrane under a strong oil-membrane attraction. In comparison, the receding force curve of the dense PVA/PVDF Janus membrane was flat because the entire oil droplet detached from the membrane surface in the absence of oil-membrane attraction. After the oil-membrane separation, the force curves of both membranes remained flat due to the lack of oil-membrane interaction. However, for the PVDF membrane, the receding force did not overlap with the advancing force curve because a large portion of the oil droplet remained on the membrane surface (Figure S5 in Supporting Information).

The oil-membrane interactions measured using oil-probe force spectroscopy provides insights to the mechanism of fouling resistance with the dense PVA/PVDF Janus membrane as illustrated in Figure 5D. For the PVDF membrane, driven by the strong hydrophobic attraction between the oil droplets and the membrane, the oil droplets in the feed solution readily attach onto the membrane surface and block the membrane pores, consequently resulting in severe membrane fouling. For the dense PVA/PVDF Janus membrane, the hydration layer on the highly hydrophilic

PVA surface deters the adhesion of the oil droplets onto the membrane surface and thereby mitigates oil fouling in the MD process.

Membrane. DCMD tests using a saline feed containing both mineral oil and SDS surfactant were conducted with the pristine PVDF membrane and dense PVA/PVDF Janus membrane. As shown in Figure 6A, the PVDF membrane could maintain a stable performance for only ~15 min. After 15 min, the normalized vapor flux significantly increased, while the salt rejection substantially decreased, indicating the occurrence of severe membrane wetting. According to our previous discussion, wetting of the PVDF membrane is induced by SDS that reduces the surface tension of the feed and the LEP of the membrane pores. Interestingly, different from the fouling test (Figure 4A), the mineral oil in the feed did not lead to an observable decline of vapor flux. The lack of oil fouling in the presence of SDS can be explained by the reduction of interfacial tension between oil and water, which effectively renders the oil droplet hydrophilic and not being able to spread on the membrane.¹⁰

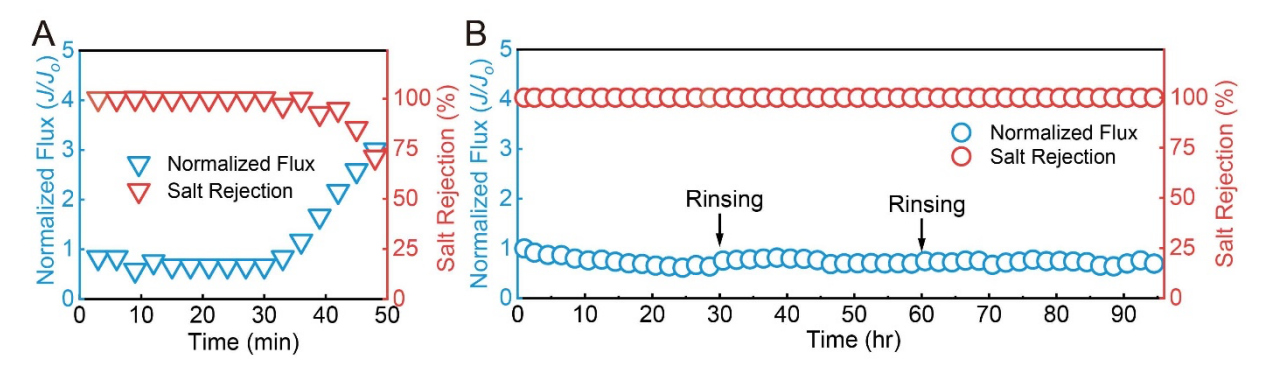


Figure 6. Simultaneous wetting and fouling resistance of the dense PVA/PVDF Janus membrane. Normalized vapor flux, J/J_0 (blue left vertical axis), and salt rejection rate (red right vertical axis) for (A) the pristine PVDF membrane and (B) dense PVA/PVDF Janus membrane in DCMD tests using feed containing 35 g/L NaCl, 1,000 ppm mineral oil, and 0.1 mM SDS. The feed and permeate temperatures were set at 60 and 20 °C, respectively, while the flow rates of feed and permeate streams were controlled at 0.8 L/min and 0.4 L/min, respectively. For the DCMD test using the dense PVA/PVDF membrane, the membrane was rinsed every 30 hours using DI water. The initial vapor fluxes in panels (A) and (B) were 23.33 \pm 3.33 and 24.00 \pm 2.66 L m⁻² h⁻¹, respectively.

In contrast, the dense PVA/PVDF Janus membrane simultaneously resisted membrane wetting and fouling, evidenced by nearly 100 % salt rejection and a relatively stable vapor flux during a prolonged DCMD experiment of 100 hours (Figure 6B). Based on the previous discussion, the

SDS surfactant cannot reach the PVDF substrate of the PVA/PVDF membrane as it cannot penetrate through the dense PVA layer, which provides highly robust wetting resistance in the prolonged MD experiments. As the SDS-containing feed solution cannot penetrate through the PVA layer but water continues to evaporate, the accumulation of SDS in the dense PVA layer would eventually reach a steady state in which advective transport of SDS into the PVA matrix is offset by the diffusive transport of SDS back to the feed solution.

In the first 30 hours of the prolonged DCMD experiment with the PVA/PVDF membrane, the vapor flux slightly decreased as the oil accumulated at the membrane surface. After rinsing with DI water, the vapor flux was restored, suggesting that the oil can be easily washed off from the membrane surface (Figure 6B). This experimental observation corroborates the previous discussion that the oil droplets did not attach to the PVDF membrane substrate due to the presence of the dense PVA layer. Such a dense hydrophilic layer both substantially delayed fouling, and more importantly, rendered fouling reversible upon washing, which is critical to sustaining a robust MD operation.

IMPLICATIONS

Conventional hydrophobic membranes are prone to membrane wetting and fouling, which significantly constrains practical MD applications. In this study, we demonstrate a simple and highly effective approach of mitigating wetting and fouling by fabricating a Janus MD membrane via applying a single dense layer of PVA onto commercial PVDF membrane. While coating hydrophobic membrane with a hydrophilic layer for fouling mitigation is not new and the use of a dense hydrophilic layer for preventing wetting has also been very recently suggested, the approach demonstrated in this study is by far the simplest and most scalable to achieve simultaneous fouling and wetting resistance. Even more importantly, the current study elucidates, for the first time, the most probable mechanism of wetting resistance imparted by a dense hydrophilic layer. This new approach to achieve wetting resistance fundamentally differs from, and is likely far more robust than, that offered by omniphobic membranes. We believe that this new approach of achieving simultaneous wetting and fouling resistance will not only provide a pathway for designing highly operationally robust MD membranes but also inspire the development of novel membranes for the separation of low-surface-tension organic solvents (e.g., ethanol and ethylene glycols).

ACKNOWLEDGEMENTS

- 504 This work was supported by the Program for Guangdong Introduction of Innovative and
- Entrepreneurial Teams (2019ZT08L213) and the US National Science Foundation (1903685).

506

507

503

SUPPORTING INFORMATION

- Detailed Procedures of Mean Pore Size and Pore Size Distribution Measurements (Figure S1);
- 509 Details of Direct Contact Membrane Distillation (DCMD) Experiments (Figure S2); DCMD
- Fouling Test Using the PVDF Membrane with Feed Containing Humic Acid (Figure S3); Oil
- Droplet Size Distribution (Figure S4); Details of Force Spectroscopy Measurement (Figure S5);
- Details of Diffusion Experiment (Figure S6); Details of Breakthrough Pressure Determination
- 513 (Figure S7); SDS Rejection Measurement.

514

515

522

523

524

525

526527

528529

530

531

532

533

534

REFERENCES

- 516 1. Grant, S. B.; Saphores, J. D.; Feldman, D. L.; Hamilton, A. J.; Fletcher, T. D.; Cook, F. L. M.; Stewardson, M.; Sanders, B. F.; Levin, L. A.; Ambrose, R. F.; Deletic, A.; Brown, R.;
- Jiang, S. C.; Rosso, D.; Cooper, W. J.; Marusic, I., Taking the "Waste" Out of "Wastewater" for Human Water Security and Ecosystem Sustainability. *Science* **2012**, *337*, (6095), 681-686.
- 520 2. Salgot, M.; Folch, M., Wastewater treatment and water reuse. *Current Opinion in Environmental Science & Health* **2018**, *2*, 64-74.
 - 3. Deshmukh, A.; Boo, C.; Karanikola, V.; Lin, S. H.; Straub, A. P.; Tong, T. Z.; Warsinger, D. M.; Elimelech, M., Membrane distillation at the water-energy nexus: limits, opportunities, and challenges. *Energ Environ Sci* **2018**, *11*, (5), 1177-1196.
 - 4. Zuo, K. C.; Wang, W. P.; Deshmukh, A.; Jia, S.; Guo, H.; Xin, R. K.; Elimelech, M.; Ajayan, P. M.; Lou, J.; Li, Q. L., Multifunctional nanocoated membranes for high-rate electrothermal desalination of hypersaline waters (October, 10.1038/s41565-020-00777-0, 2020). *Nat Nanotechnol* **2020**, *15*, (12), 1065-1065.
 - 5. Bundschuh, J.; Ghaffour, N.; Mahmoudi, H.; Goosen, M.; Mushtaq, S.; Hoinkis, J., Lowcost low-enthalpy geothermal heat for freshwater production: Innovative applications using thermal desalination processes. *Renew Sust Energ Rev* **2015**, *43*, 196-206.
 - 6. Wang, W. B.; Shi, Y.; Zhang, C. L.; Hong, S.; Shi, L.; Chang, J.; Li, R. Y.; Jin, Y.; Ong, C.; Zhuo, S. F.; Wang, P., Simultaneous production of fresh water and electricity via multistage solar photovoltaic membrane distillation. *Nat Commun* **2019**, *10*, 3012.
- 7. Wang, Z. X.; Horseman, T.; Straub, A. P.; Yip, N. Y.; Li, D. Y.; Elimelech, M.; Lin, S. H., Pathways and challenges for efficient solar-thermal desalination. *Sci Adv* **2019**, *5*, (7), eaax0763.
- 8. Dongare, P. D.; Alabastri, A.; Pedersen, S.; Zodrow, K. R.; Hogan, N. J.; Neumann, O.;
- Wu, J. J.; Wang, T. X.; Deshmukh, A.; Elimelech, M.; Li, Q. L.; Nordlander, P.; Halas, N. J.,
- Nanophotonics-enabled solar membrane distillation for off-grid water purification. P Natl Acad
- 540 Sci USA **2017**, 114, (27), 6936-6941.

9. Rice, D.; Ghadimi, S. J.; Barrios, A. C.; Henry, S.; Walker, W. S.; Li, Q. L.; Perreault, F., Scaling Resistance in Nanophotonics-Enabled Solar Membrane Distillation. *Environ Sci Technol* **2020**, *54*, (4), 2548-2555.

- 10. Wang, Z. X.; Lin, S. H., Membrane fouling and wetting in membrane distillation and their mitigation by novel membranes with special wettability. *Water Res* **2017**, *112*, 38-47.
- 11. Horseman, T.; Yin, Y.; Christie, K. S. S.; Wang, Z.; Tong, T.; Lin, S., Wetting, Scaling, and Fouling in Membrane Distillation: State-of-the-Art Insights on Fundamental Mechanisms and Mitigation Strategies. *ACS ES&T Engineering* **2021**, *1*, (1), 117-140.
- 12. Wang, Z. X.; Chen, Y. M. L.; Sun, X. M.; Duddu, R.; Lin, S. H., Mechanism of pore wetting in membrane distillation with alcohol vs. surfactant. *J Membrane Sci* **2018**, *559*, 183-195.
- 13. Rezaei, M.; Warsinger, D. M.; Lienhard, J. H.; Duke, M. C.; Matsuura, T.; Samhaber, W. M., Wetting phenomena in membrane distillation: Mechanisms, reversal, and prevention. *Water Res* **2018**, *139*, 329-352.
- 14. Aboulhassan, M. A.; Souabi, S.; Yaacoubi, A.; Baudu, M., Removal of surfactant from industrial wastewaters by coagulation flocculation process. *International Journal of Environmental Science & Technology* **2006**, *3*, (4), 327-332.
- 15. Petrovic, M.; Gonzalez, S.; Barcelo, D., Analysis and removal of emerging contaminants in wastewater and drinking water. *Trac-Trend Anal Chem* **2003**, *22*, (10), 685-696.
- 16. Zhang, Z. Y.; Du, X. W.; Carlson, K. H.; Robbins, C. A.; Tong, T. Z., Effective treatment of shale oil and gas produced water by membrane distillation coupled with precipitative softening and walnut shell filtration. *Desalination* **2019**, *454*, 82-90.
- 17. Boo, C.; Lee, J.; Elimelech, M., Omniphobic Polyvinylidene Fluoride (PVDF) Membrane for Desalination of Shale Gas Produced Water by Membrane Distillation. *Environ Sci Technol* **2016**, *50*, (22), 12275-12282.
- 18. Israelachvili, J.; Pashley, R., The hydrophobic interaction is long range, decaying exponentially with distance. *Nature* **1982**, *300*, (5890), 341-342.
- 19. Meyer, E. E.; Rosenberg, K. J.; Israelachvili, J., Recent progress in understanding hydrophobic interactions. *P Natl Acad Sci USA* **2006**, *103*, (43), 15739-15746.
- 20. Wang, Z. X.; Elimelech, M.; Lin, S. H., Environmental Applications of Interfacial Materials with Special Wettability. *Environ Sci Technol* **2016**, *50*, (5), 2132-2150.
- 21. Chew, N. G. P.; Zhao, S. S.; Wang, R., Recent advances in membrane development for treating surfactant- and oil-containing feed streams via membrane distillation. *Advances in Colloid and Interface Science* **2019**, *273*, 102022.
- 22. Yao, M. W.; Tijing, L. D.; Naidu, G.; Kim, S. H.; Matsuyama, H.; Fane, A. G.; Shon, H. K., A review of membrane wettability for the treatment of saline water deploying membrane distillation. *Desalination* **2020**, *479*, 114312.
- 23. Chang, H.; Liu, B.; Zhang, Z.; Pawar, R.; Yan, Z.; Crittenden, J. C.; Vidic, R. D., A Critical Review of Membrane Wettability in Membrane Distillation from the Perspective of Interfacial Interactions. *Environ Sci Technol* **2021**, *55*, (3), 1395-1418.
- 581 24. Lin, S. H.; Nejati, S.; Boo, C.; Hu, Y. X.; Osuji, C. O.; Ehmelech, M., Omniphobic 582 Membrane for Robust Membrane Distillation. *Environ Sci Tech Let* **2014**, *1*, (11), 443-447.
- 583 25. Lu, K. J.; Chen, Y. M. L.; Chung, T. S., Design of omniphobic interfaces for membrane distillation A review. *Water Res* **2019**, *162*, 64-77.

26. Chew, N. G. P.; Zhao, S. S.; Malde, C.; Wang, R., Polyvinylidene fluoride membrane modification via oxidant-induced dopamine polymerization for sustainable direct-contact membrane distillation. *J Membrane Sci* **2018**, *563*, 31-42.

- 27. Zuo, G. Z.; Wang, R., Novel membrane surface modification to enhance anti-oil fouling property for membrane distillation application. *J Membrane Sci* **2013**, *447*, 26-35.
- 28. Wang, Z. X.; Hou, D. Y.; Lin, S. H., Composite Membrane with Underwater-Oleophobic Surface for Anti-Oil-Fouling Membrane Distillation. *Environ Sci Technol* **2016**, *50*, (7), 3866-3874.
- 29. Deka, B. J.; Guo, J. X.; Khanzada, N. K.; An, A. K., Omniphobic re-entrant PVDF membrane with ZnO nanoparticles composite for desalination of low surface tension oily seawater. *Water Res* **2019**, *165*, 114982.
- 30. Huang, Y. X.; Wang, Z. X.; Jin, J.; Lin, S. H., Novel Janus Membrane for Membrane Distillation with Simultaneous Fouling and Wetting Resistance. *Environ Sci Technol* **2017**, *51*, (22), 13304-13310.
- 31. Li, C. X.; Li, X. S.; Du, X. W.; Tong, T. Z.; Cath, T. Y.; Lee, J., Antiwetting and Antifouling Janus Membrane for Desalination of Saline Oily Wastewater by Membrane Distillation. *Acs Appl Mater Inter* **2019**, *11*, (20), 18456-18465.
- 32. Cornelis, G.; Boussu, K.; Van der Bruggen, B.; Devreese, I.; Vandecasteele, C., Nanofiltration of Nonionic Surfactants: Effect of the Molecular Weight Cutoff and Contact Angle on Flux Behavior. *Ind Eng Chem Res* **2005**, *44*, (20), 7652-7658.
- 33. Boussu, K.; Kindts, C.; Vandecasteele, C.; Van der Bruggen, B., Surfactant fouling of nanofiltration membranes: Measurements and mechanisms. *Chemphyschem* **2007**, *8*, (12), 1836-1845.
- 34. Chen, Y.; Lu, K.-J.; Gai, W.; Chung, T.-S., Nanofiltration-Inspired Janus Membranes with Simultaneous Wetting and Fouling Resistance for Membrane Distillation. *Environ Sci Technol* **2021**, *55*, (11), 7654-7664.
- 35. Xue, Y. L.; Huang, J.; Lau, C. H.; Cao, B.; Li, P., Tailoring the molecular structure of crosslinked polymers for pervaporation desalination. *Nat Commun* **2020**, *11*, (1), 1461.
- 36. Boo, C.; Hong, S.; Elimelech, M., Relating Organic Fouling in Membrane Distillation to Intermolecular Adhesion Forces and Interfacial Surface Energies. *Environ Sci Technol* **2018**, *52*, (24), 14198-14207.
- 37. Hou, D. Y.; Wang, Z. X.; Wang, K. P.; Wang, J.; Lin, S. H., Composite membrane with electrospun multiscale-textured surface for robust oil-fouling resistance in membrane distillation. *J Membrane Sci* **2018**, *546*, 179-187.
- 38. Wang, K. P.; Hou, D. Y.; Wang, J.; Wang, Z. X.; Tian, B. H.; Liang, P., Hydrophilic surface coating on hydrophobic PTFE membrane for robust anti-oil-fouling membrane distillation. *Appl Surf Sci* **2018**, *450*, 57-65.
- 39. Zhou, X. C.; Wang, Z. X.; Epsztein, R.; Zhan, C.; Li, W. L.; Fortner, J. D.; Pham, T. A.; Kim, J. H.; Elimelech, M., Intrapore energy barriers govern ion transport and selectivity of desalination membranes. *Sci Adv* **2020**, *6*, (48), eabd9045.
- 40. Pan, F. S.; Jia, H. P.; Jiang, Z. Y.; Zheng, X. H.; Wang, J. T.; Cui, L., P(AA-626 AMPS)-PVA/polysulfone composite hollow fiber membranes for propylene dehumidification. *J Membrane Sci* **2008**, *323*, (2), 395-403.
- 628 41. Garcia-Payo, M. C.; Izquierdo-Gil, M. A.; Fernandez-Pineda, C., Wetting study of 629 hydrophobic membranes via liquid entry pressure measurements with aqueous alcohol solutions. *J Colloid Interf Sci* **2000**, *230*, (2), 420-431.

42. Jacob, P.; Laborie, S.; Cabassud, C., Visualizing and evaluating wetting in membrane distillation: New methodology and indicators based on Detection of Dissolved Tracer Intrusion (DDTI). *Desalination* **2018**, *443*, 307-322.

- 43. Chanachai, A.; Meksup, K.; Jiraratananon, R., Coating of hydrophobic hollow fiber PVDF membrane with chitosan for protection against wetting and flavor loss in osmotic distillation process. *Sep Purif Technol* **2010**, *72*, (2), 217-224.
- 44. Qtaishat, M.; Rana, D.; Khayet, M.; Matsuura, T., Preparation and characterization of novel hydrophobic/hydrophilic polyetherimide composite membranes for desalination by direct contact membrane distillation. *J Membrane Sci* **2009**, *327*, (1), 264-273.
- 45. Bonyadi, S.; Chung, T. S., Flux enhancement in membrane distillation by fabrication of dual layer hydrophilic—hydrophobic hollow fiber membranes. *J Membrane Sci* **2007**, *306*, (1), 134-146.
- 46. Chen, Y.; Lu, K.-J.; Japip, S.; Chung, T.-S., Can Composite Janus Membranes with an Ultrathin Dense Hydrophilic Layer Resist Wetting in Membrane Distillation? *Environ Sci Technol* **2020**, *54*, (19), 12713-12722.
- 47. Wang, Z. X.; Chen, Y. M. L.; Lin, S. H., Kinetic model for surfactant-induced pore wetting in membrane distillation. *J Membrane Sci* **2018**, *564*, 275-288.
- 48. Wang, Z. X.; Chen, Y. M. L.; Zhang, F. Y.; Lin, S. H., Significance of surface excess concentration in the kinetics of surfactant-induced pore wetting in membrane distillation. *Desalination* **2019**, *450*, 46-53.
- 49. Gong, G. H.; Wang, P.; Zhou, Z. Y.; Hu, Y. X., New Insights into the Role of an Interlayer for the Fabrication of Highly Selective and Permeable Thin-Film Composite Nanofiltration Membrane. *Acs Appl Mater Inter* **2019**, *11*, (7), 7349-7356.
- 50. Tuller, M.; Or, D.; Dudley, L. M., Adsorption and capillary condensation in porous media: Liquid retention and interfacial configurations in angular pores. *Water Resour Res* **1999**, *35*, (7), 1949-1964.
- 51. Liu, H. L.; Cao, G. X., Effectiveness of the Young-Laplace equation at nanoscale. *Sci Rep-Uk* **2016**, *6*, 23936.
- 52. Mo, J. W.; Sha, J. J.; Li, D. K.; Li, Z. G.; Chen, Y. F., Fluid release pressure for nanochannels: the Young-Laplace equation using the effective contact angle. *Nanoscale* **2019**, *11*, (17), 8408-8415.
- 53. Chen, S. F.; Li, L. Y.; Zhao, C.; Zheng, J., Surface hydration: Principles and applications toward low-fouling/nonfouling biomaterials. *Polymer* **2010**, *51*, (23), 5283-5293.

666 TOC Art

